

Lawrence Berkeley National Laboratory

LBL Publications

Title

Laboratory system for studying cryogenic thermal rock fracturing for well stimulation

Permalink

<https://escholarship.org/uc/item/4zq9426t>

Authors

Cha, Minsu
Alqahtani, Naif B
Yin, Xiaolong
[et al.](#)

Publication Date

2017-07-01

DOI

10.1016/j.petrol.2017.06.062

Peer reviewed

Laboratory system for studying cryogenic thermal rock fracturing for well stimulation

Author links open overlay panel [MinsuCha^a](#) [Naif B. Alqahtani^b](#) [Xiaolong Yin^c](#) [Timothy J. Kneafsey^d](#) [Bowen Yao^e](#) [Yu-Shu Wu^e](#)

Show more

<https://doi.org/10.1016/j.petrol.2017.06.062> Get rights and content

Highlights

-

A laboratory system for cryogenic fracturing under true-triaxial loading is developed.

-

Cryogen is flown through boreholes by a coaxial assembly under controlled pressure.

-

Designs for physical parameter measurements at cryogenic temperatures are optimized.

-

Acoustic, pressure decay, and breakdown tests effectively capture cryogenic fractures.

-

Data shows the laboratory design works adequately for cryogenic stimulation studies.

Abstract

The concept of [cryogenic](#) fracturing is that a sharp thermal gradient developed by applying a cryogenic fluid on a rock surface causes a strong local [tensile stress](#) that initiates fractures. Prior [field tests](#) suggest that field application with special equipment rated for cryogenic temperatures may deliver potential benefits. The tests did not, however, identify the fracture mechanisms at work in downhole conditions. In this study, we present our laboratory designs and procedures developed for studying cryogenic fracturing mechanisms in a well environment, and examine typical data indicative of the performance of the system. The [experimental apparatus](#) and procedures were

specifically designed to conduct cryogenic fracturing tests in specimens under confining stress, with integrated cryogen transport, measurements, and fracture characterization. A true-triaxial loading system was built to simulate reservoir stress levels and anisotropic stress application, and was designed to avoid [thermal stresses](#) in tests involving cryogen by arranging discrete components in an open chamber. To maximize [thermal shock](#) on the wellbore surface, tubing and [wellhead](#) are configured so that [liquid nitrogen](#) enters the [borehole](#) and flow out after contributing to thermal shock. The temperature at boreholes and along flow lines, borehole pressure, and liquid nitrogen consumption are monitored throughout treatments. [Acoustic](#) transmission and pressure-decay measurements are used to characterize fractures before and after the experiments. Breakdown tests performed on un-stimulated specimens and stimulated specimens compare breakdown pressures of the two groups and thus evaluate the performance of thermal fracturing. The laboratory design was able to effectively apply cryogenic stimulations to laboratory rock specimens. The characterization methods were able to capture fracture creation and rock property changes due to cryogenic fracturing.

Keywords

Cryogenic rock fracturing

Thermal shock

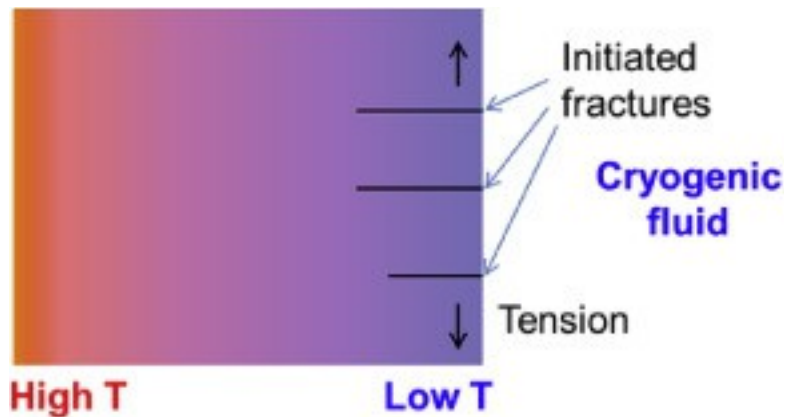
Well stimulation

Laboratory development

Shale and tight gas reservoirs

1. Introduction

[Cryogenic](#) fracturing is based on the idea that a cold fluid induces thermal fractures when brought into contact with a much warmer rock. When [liquid nitrogen](#) as a cryogen is injected into a [borehole](#) in rock with much higher temperature, the heat from the rock will quickly transfer to the cryogenic fluid. This rapid heat transfer, better known as a [thermal shock](#), will cause the surface of the rock to contract and fail in tension, thus inducing fractures orthogonal to the contact plane of the cryogen and rock ([Fig. 1](#)).



1. [Download high-res image \(114KB\)](#)
2. [Download full-size image](#)

Fig. 1. The basic concept of [cryogenic](#) fracturing.

Hydraulic fracturing uses water-based fluids due to general availability and low cost; however, a heavy dependence on water presents a number of disadvantages. Water can cause significant formation damage, resulting from [clay swelling](#) in the wetted rock, and relative permeability effects stemming from capillary fluid retention ([Mazza, 1997](#)). The formation damage mechanisms inhibit [hydrocarbon](#) flow and impair production rates and recovery efficiency. Also, water used in large quantities may place stress upon the local environments where fracturing activities occur. Finally, downhole injection of chemicals needed in water-based fracturing operations, including slickwater and gel, are environmentally controversial ([Stringfellow et al., 2014](#)). In these aspects, cryogenic fracturing has the potential to offer benefits ([Wang et al., 2016](#)).

Cryogenic fracturing using liquid nitrogen can achieve extremely low temperatures and very strong thermally induced stresses. [Grundmann et al. \(1998\)](#) treated a [Devonian shale](#) well with liquid nitrogen and observed an initial production rate 8% higher than the rate in a nearby offset well that had undergone traditional fracturing with nitrogen gas. Unfortunately, subsequent production information was unavailable because the well had to be shut in for logistical reasons. To further advance the study of cryogen fluids on hydrocarbon producing formations, [McDaniel et al. \(1997\)](#) conducted simple laboratory studies where [coal](#) samples were immersed in cryogenic nitrogen. The coal samples experienced significant shrinkage and fractured into smaller cubic units, with the creation of microfractures orthogonal to the surface exposed to the cold fluid. The researchers found that repeated exposure cycles to the cryogen caused the coal to break into smaller and smaller pieces, becoming rubblized. After three cycles of exposing the coal to liquid nitrogen and subjecting the coal to [ambient temperature](#), the coal block was fractured to [grain size](#) particles. [McDaniel et al. \(1997\)](#) also

conducted [field experiments](#) by re-stimulating four [coal-bed methane](#) (CBM) wells and one tight [sandstone](#) well with liquid nitrogen. The wells were retrofitted with stainless steel surface piping, manifolds, and [wellhead](#) component to prevent thermal contraction problems. Free-hanging [fiberglass](#) tubing was used to transport the liquid nitrogen to the target formations in order not to compromise the casing integrity. The results were mixed: all five wells showed promising re-stimulation initial production rates 10–20 times the before-re-stimulation production average; however, those rates quickly dwindled. The CBM wells showed sustained six-month re-stimulation production increases of 0–45%. The tight sand well initially had higher flow rates for two months after re-stimulating, but then had a 65% loss in production from pre re-stimulation performance. It is thought that the initial success in re-stimulating these wells is attributed to the fact that the damage from the gel [filter cake](#) of previous fracturing treatments was reduced. These studies indicate that fracturing with liquid nitrogen may be viable for the field and bring benefits in reducing formation damage, water, and chemical use. However, when it comes to an understanding of cryogenic fracturing mechanisms, few lab studies have been done to systematically investigate processes. Research is required to better understand the mechanisms of cryogenic fracturing processes under controlled environments and how they can be integrated into our current fracturing practices if cryogenic fracturing potential is proven to be high.

Proper design of [laboratory equipment](#) is important to effectively investigate cryogenic fracturing processes. Here, we developed a laboratory system for cryogenic fracturing under true-triaxial loading conditions. It allows characterization of cryogenic fracturing processes in the laboratory under controlled conditions, such as anisotropic loading conditions and different cryogenic fracturing schemes. The devices and procedures have been improved and optimized based on our understanding cryogen and system behavior from our preliminary studies including [Cha et al., 2014](#), [Cha et al., 2016](#).

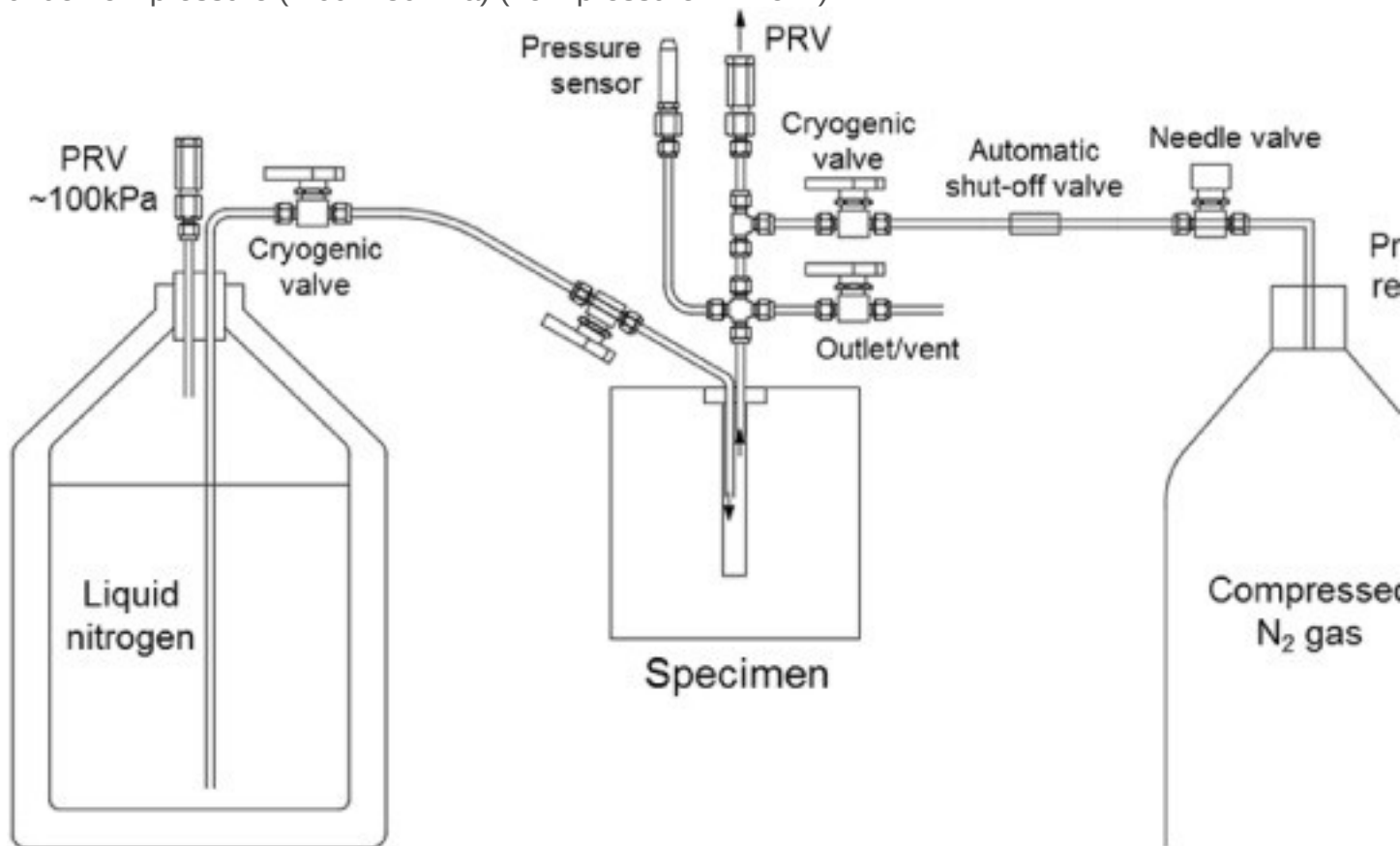
2. Devices for cryogenic stimulation experiments

The laboratory system consists of a triaxial loading device, a [liquid nitrogen](#) (LN) delivery and flow-through system, and measurement/characterization systems. Compressed nitrogen gas was used to either directly pressurize [boreholes](#) or to push liquid nitrogen into boreholes at higher pressure. Cryogen submersion tests and unconfined tests are not included in this article but are detailed in [Cha et al. \(2014\)](#).

2.1. Cryogen delivery

The cryogen transport lines should be able to withstand temperatures down to $-196\text{ }^{\circ}\text{C}$. Stainless steel 316 and brass generally provide such an ability because their brittleness-ductility [transition temperature](#) is lower than the normal liquid nitrogen [boiling point](#). However, stainless steel has a higher pressure rating at the temperature. Also, tubing used for liquid nitrogen flow under elevated pressure needs to be seamless and annealed.

From the liquid nitrogen (LN) dewar, LN was released by internal gas nitrogen pressure generated inside the dewar once an outlet was opened. This pressure was kept at relatively low levels $\sim 60\text{--}130\text{ kPa}$ (gage pressure) inside a dewar by a pressure [relief valve](#) (PRV) ([Fig. 2](#)). The [fluid injection](#) system for [cryogenic](#) fracturing is fundamentally different from that for hydraulic fracturing because cryogenic fluid needs to keep flowing in order to cool the borehole down. Stagnant liquid nitrogen in the borehole would quickly boil and vaporize. [Fig. 2](#) shows the system where LN was flowed directly from the dewar to the specimen borehole and nitrogen gas flows out through an outlet vent under low pressure ($\sim 60\text{--}130\text{ kPa}$) (“low-pressure LN flow”).



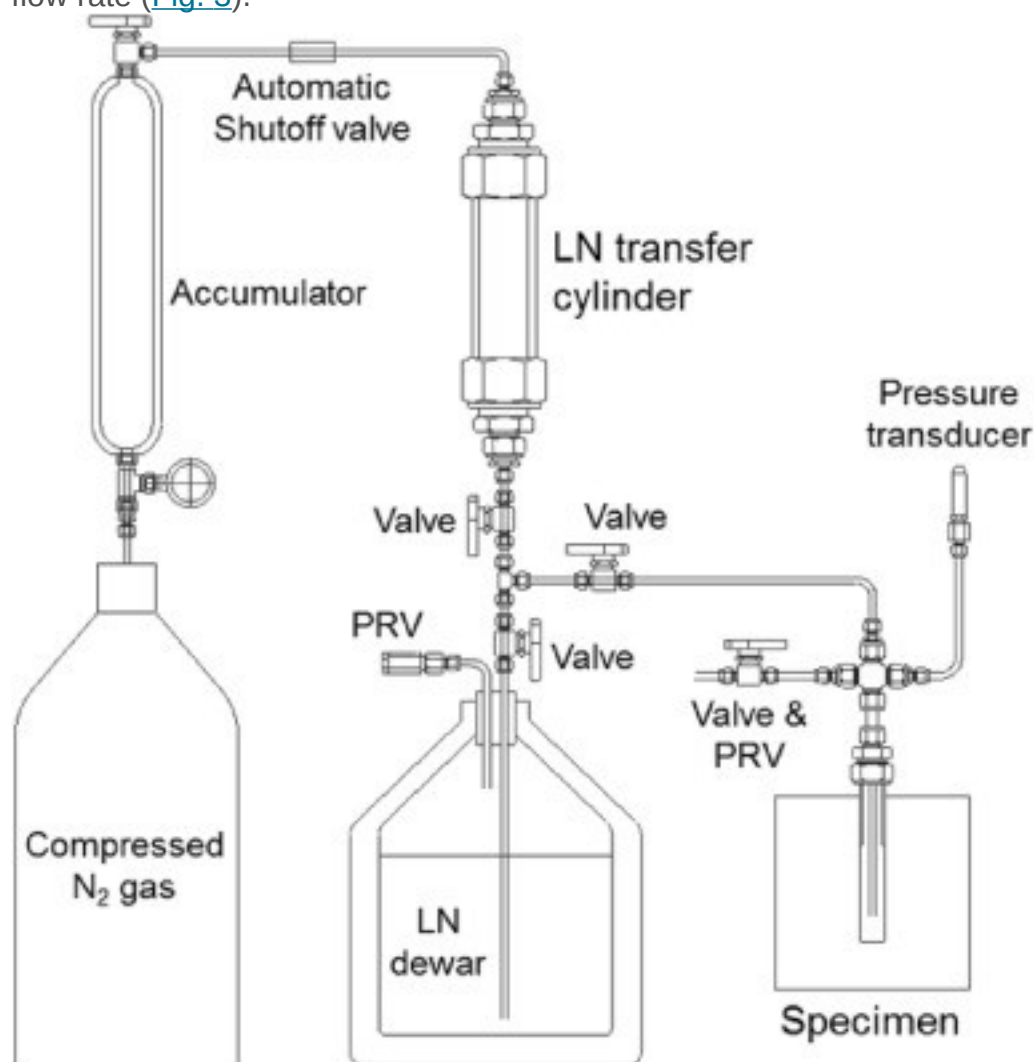
1. [Download high-res image \(281KB\)](#)
2. [Download full-size image](#)

Fig. 2. Basic schematic of lab [cryogenic](#) stimulation setup under low-pressure LN flow (the triaxial loading device not shown). Compressed nitrogen gas can be used to pressurize [boreholes](#).

Following cryogen flows, boreholes may be pressurized by gaseous nitrogen (GN) as a part of a [well stimulation](#) to help propagate fractures created by [thermal shock](#).

Compressed nitrogen gas was also used to pressurize boreholes for breakdown tests in order to evaluate stimulation performance as discussed in Sections [3 Experimental procedure](#), [4.2 Fracture assessment and characterization](#). Nitrogen [gas pressure](#) can be applied from the gas cylinder as shown on the right-hand side of [Fig. 2](#).

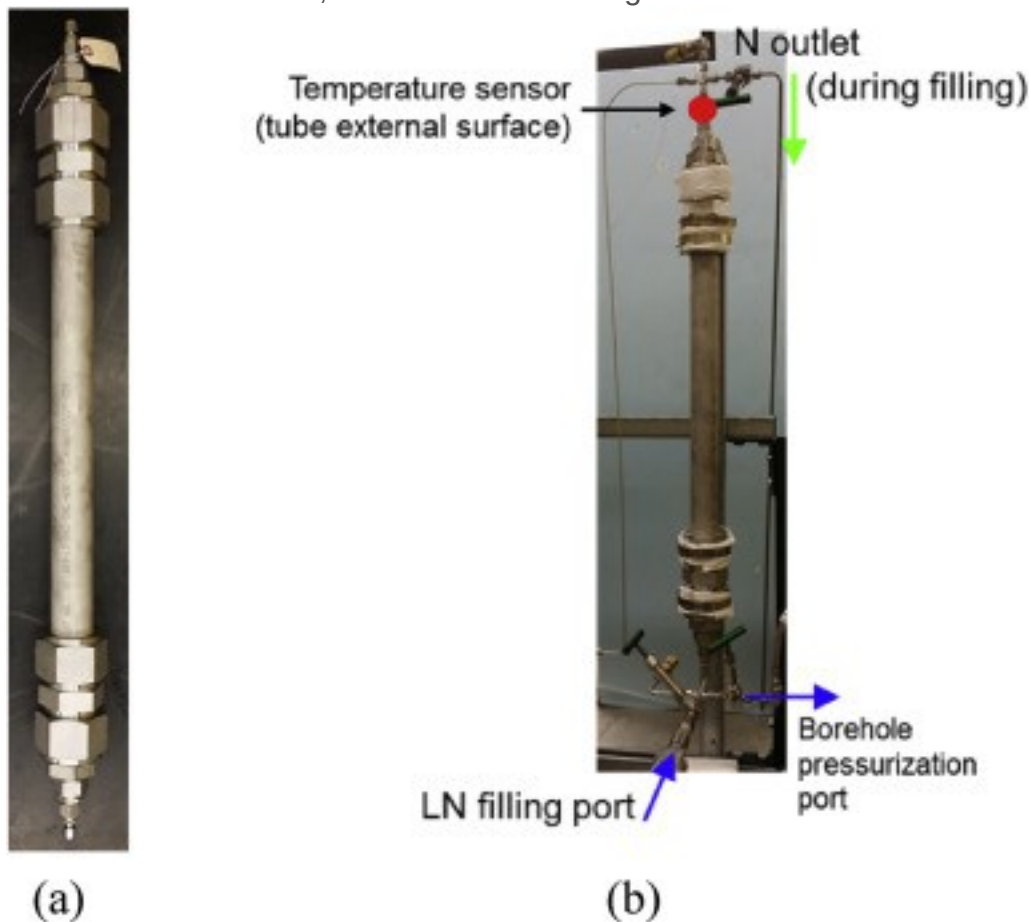
In order to flow LN under higher pressure and flow rate, it needs to be temporarily stored in a transfer cylinder, as the dewar cannot accommodate elevated pressure ([Fig. 3](#)). Then compressed gaseous nitrogen pressure was applied to the top end of the vessel to push LN into the borehole from the bottom end, under higher pressure and flow rate ([Fig. 3](#)).



1. [Download high-res image \(253KB\)](#)
2. [Download full-size image](#)

Fig. 3. Schematic of lab [cryogenic](#) stimulation setup for higher-pressure LN flow. LN is temporarily stored in the transfer cylinder from the dewar, and compressed nitrogen gas is used to push LN to specimen [boreholes](#).

The transfer cylinder was made of annealed seamless stainless steel tubing with outside diameter (OD) of 5.1 cm, inside diameter (ID) of 4.1 cm, and length of 70 cm. The 5.1 cm-OD tubing was reduced to the 0.64 cm-OD tubing by multi-stage reductions of tube fittings ([Fig. 4](#)). The vessel tubing is rated for 7 MPa at [ambient temperature](#), but downrated to 3.5 MPa at cryogenic temperature. The vessel was heavily insulated to minimize heat transfer, and its internal storage volume is 1 L.



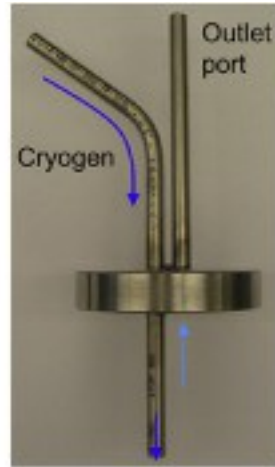
1. [Download high-res image \(275KB\)](#)
2. [Download full-size image](#)

Fig. 4. [Liquid nitrogen](#) transfer cylinder for higher-pressure LN flow. (a) 5.1 cm-OD stainless steel tubing. (b) Assembled to the system. (Photo taken before applying insulation).

In field applications, heat loss and integrity of transport lines and casing may be issues to overcome for delivery of liquid nitrogen to the downhole environment. For both vertical and horizontal wells, injection pipe string should have minimum contact with the casing in order to not affect casing integrity and to minimize heat loss. The injection pipes should maintain sufficient strength and structural integrity at cryogenic temperature. Suitable materials include stainless steel, brass, and [fiberglass](#) ([Wilson et al., 1995](#)). Fiberglass has the merit of a lower cost, and lighter weight, and lower [thermal conductivity](#), and for these reasons was tried in [field tests](#) ([McDaniel et al., 1997](#)). Due to inherent heat loss, the delivery pipe should be cooled before the cryogen can flow in a [liquid state](#). From our laboratory experience, faster flow rate helps overall thermal flux, reducing the relative rate of heat loss. Nevertheless, heat loss is inevitable and may increase at greater depth. In-situ cooling may be a potential alternative, such as by Joule-Thomson process, which requires development.

2.2. Borehole packing/sealing and flow-through

As mentioned earlier, unlike pressure-induced fracturing, e.g., hydraulic fracturing, cryogen needs to keep flowing through a borehole in order to cool the borehole down. A reasonable flow rate of cryogen is required to cool the borehole, either by a circulation path to the outside of the borehole or by leakoff through existing or newly created fractures. The latter is difficult because we are mainly targeting low-permeability formations. To achieve a cryogen flow-through path, we devised two methods. The first one was placing a packer at the entrance of the borehole ([Fig. 2](#), [Fig. 5](#)). The packer has inlet and outlet tubes built into it. A gasket was used to seal between packers and the surface around boreholes. Some force was applied on top of the packer, by a load plate to induce a pressure-seal between the sample and the packer/gasket. We used PTFE sheets for [gaskets](#), which resist temperatures down to $-212\text{ }^{\circ}\text{C}$. Any uneven surfaces on the gasket seat were filled by epoxy to provide good contact and seal between gasket and specimen surface ([Fig. 5b](#)). The packer was moderately effective for low borehole pressure applications, but it allowed leakage through contacts at higher borehole pressure during higher-pressure LN flow tests and pressure decay tests.

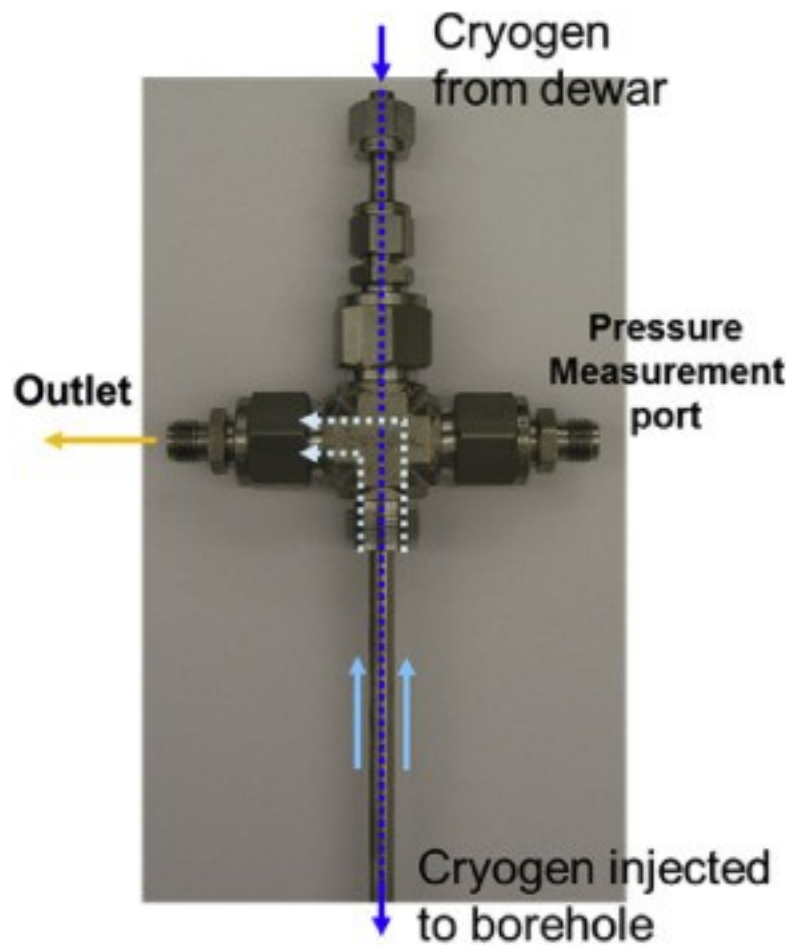


(a) Packer with inlet and outlet tubings (b) Silicone pad, packer and PTFE gasket

1. [Download high-res image \(294KB\)](#)
2. [Download full-size image](#)

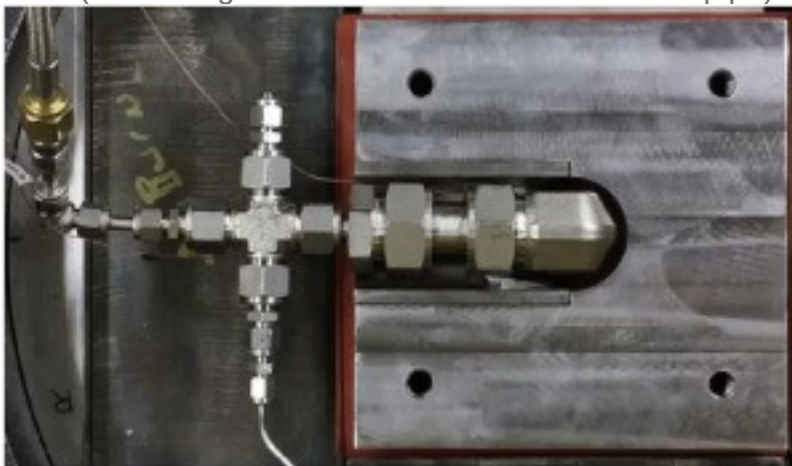
Fig. 5. [Borehole](#) sealing and flow-through by a packer with an inlet and outlet.

In the second method, a casing was mounted in the borehole, which turned out to be a robust solution for longer stimulations and/or higher-pressure stimulations. This method is also more applicable to field implementation. A 2.5-cm OD stainless steel tube used as a borehole casing was inserted 5 cm into the borehole and mounted to the borehole wall using epoxy to seal and resist [fluid pressure](#). Epoxy generally performed well during cryogenic stimulations, but could deteriorate after 3–5 cycles. To allow flow, we developed an innovative design that enables effective flow through a coaxial inlet and outlet ([Fig. 6](#), [Fig. 7](#)). Cryogen enters the borehole through the central smaller-diameter inlet tubing (blue line and arrows in [Fig. 6](#)), which passes through a larger-size cross-shaped fitting. Then warmed nitrogen exits through the [annulus](#) between the inlet tubing and the casing, and then through the space in the cross fitting ([Fig. 6](#)). For confined specimen tests, an elbow was used to accommodate vertical loading piston ([Fig. 7](#)). One advantage of the coaxial assembly was more area inside the casing is utilized for flow through so that broader range of flow rates can be controlled using an outlet valve. Insulation was applied to all transport lines from the dewar to the specimen inlet to minimize heat loss.



1. [Download high-res image \(277KB\)](#)
2. [Download full-size image](#)

Fig. 6. Coaxial design for cryogen flow through the [borehole](#) – for unconfined specimen tests (the casing detached to show the inner inlet pipe).



1. [Download high-res image \(448KB\)](#)
2. [Download full-size image](#)

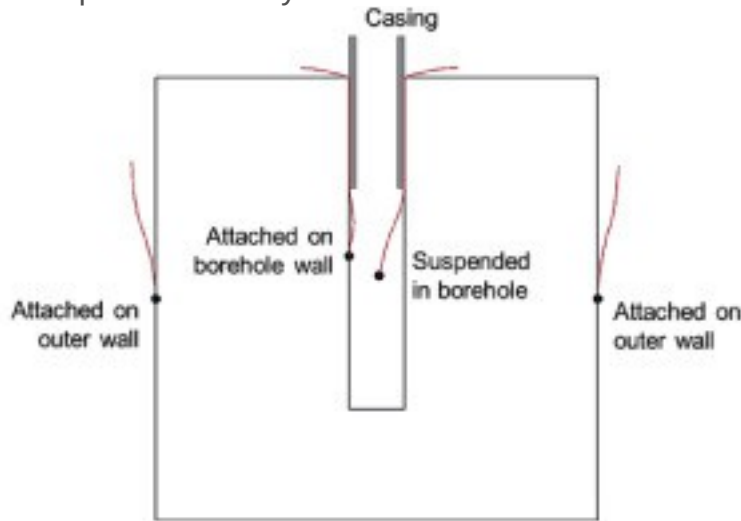
Fig. 7. Setup for coaxial cryogen flow through – for confined specimen tests.

2.3. Measurements

Monitoring during stimulation includes pressure, temperature, and liquid nitrogen consumption. Pre- and post-stimulation measurements relevant to fracture characterization include photography of specimens, [acoustics](#), pressure decay, and breakdown pressure levels.

2.3.1. Temperature measurement

Temperature measurements are critical to observe system performance and behavior. T-type [thermocouples](#) (TC) were selected for range and accuracy. Temperatures are measured at the borehole wall surface and borehole space, and at two outer surfaces ([Fig. 8a](#)). For the measurements inside a borehole, two thin thermocouples were placed into the borehole first before applying gaskets and packers ([Fig. 8b](#)). Then, packers were loaded by the top load platen to create a tight seal. When using casing, thermocouple wires were inserted into borehole between casing and borehole walls ([Fig. 8a](#)). The thermocouple suspended in the borehole recorded temperature in the borehole space and thus informed us of nitrogen phase state, and the thermocouple attached to the borehole wall better measures the temperature at the rock surface ([Fig. 8](#)). Gas in the borehole leaked through minute gaps between TC and its plastic coating, especially at higher borehole pressures during breakdown tests and pressure decay tests. Therefore, the borehole ends of TCs need to be sealed to avoid leakage and not to affect pressure decay results.



(a) Locations of thermocouple tips in a block



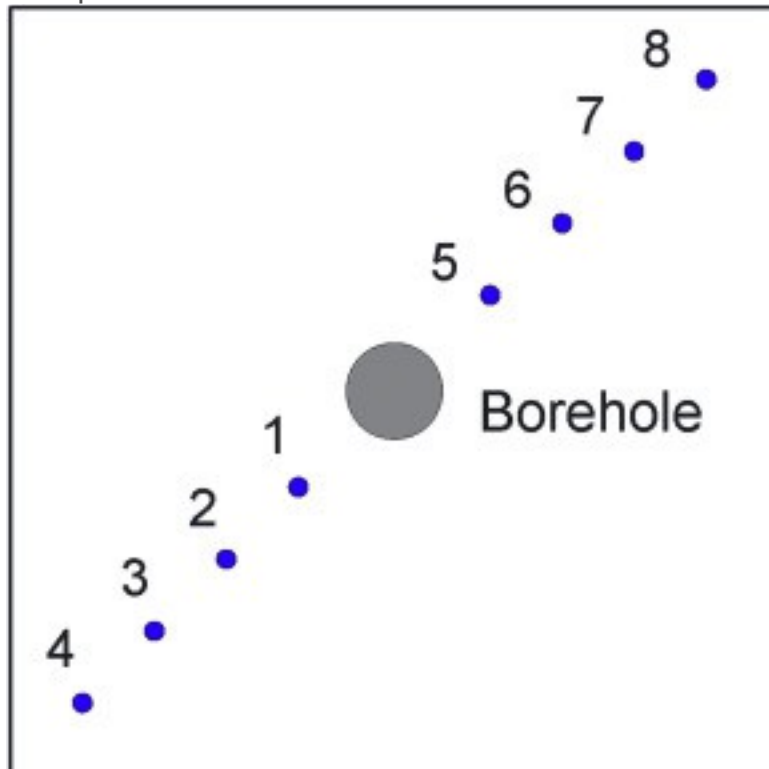
(b) TC attached to borehole wall

1. [Download high-res image \(251KB\)](#)
2. [Download full-size image](#)

Fig. 8. [Thermocouple](#) instrumentation on a test block.

To quantify temperature propagation inside specimens during thermal stimulation, an array of thermocouples was embedded inside a concrete block for a few selected specimens. Thin thermocouples (0.1 mm in diameter) were embedded on the diagonal in the concrete specimen at mid-height while the concrete was fresh ([Fig. 9](#)).

Temperatures were also measured in the outlet and several points along cryogenic transport lines.



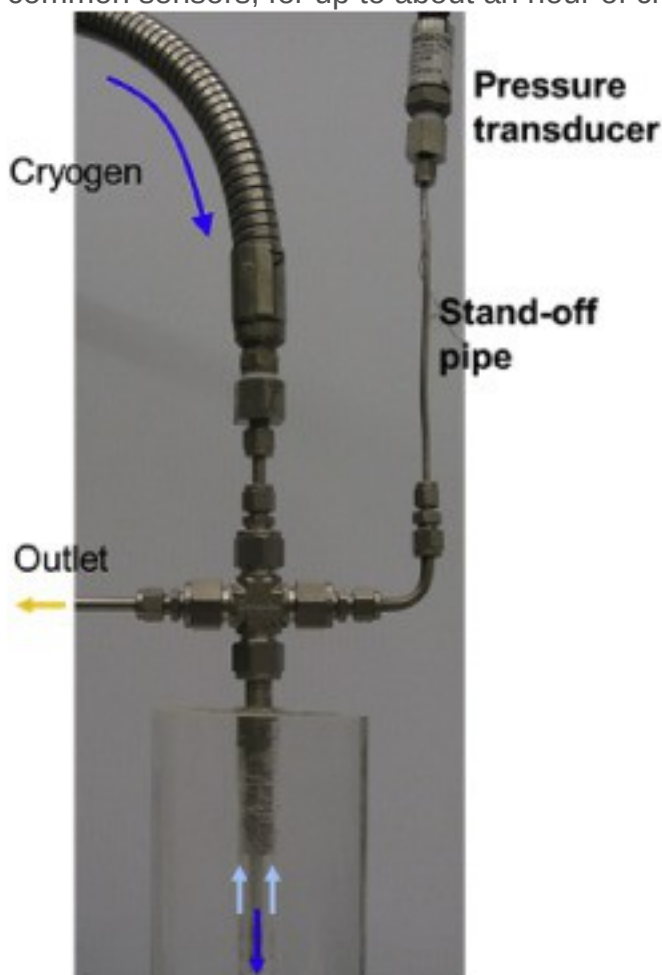
1. [Download high-res image \(89KB\)](#)
2. [Download full-size image](#)

Fig. 9. Locations of TC tips inside a concrete block at its mid-height for temperature measurements.

2.3.2. Pressure measurements

Monitoring fluid pressure in the borehole is necessary to properly understand the system behavior as well as for safety. Pressure and temperature are intimately coupled to each other, and this is more apparent in an environment that experiences large and rapid changes in temperature and fluid pressure in a relatively closed system. Operating a pressure transducer at cold temperature or exposing the sensor to cryogenic fluid will

damage sensing elements of most pressure transducers, and cryogenic-rated pressure sensors that are designed to work in such an environment are costly. In this study, borehole pressure is measured using a regular pressure transducer by attaching it to the end of a vertical standoff pipe connected to the flow line ([Fig. 10](#)). There is no flow in the standoff pipe, and a stagnant vapor [cushion](#) is created that prevents the cold temperature from affecting the sensor. The temperature at the top of the stand-off pipe was measured and remained above 0 °C throughout the stimulation ([Fig. 17b](#)). The standoff pipe length should not be longer than necessary because a long narrow pipe can create drag force and thus may decrease responsiveness to any fast-changing pressure. The length of a standoff pipe can be reduced by decreasing the diameter of the pipe because of better heat dissipation in pipes with a smaller diameter. It was found that stand-off pipe length as short as 10 cm was sufficient to keep the top end of the stand-off pipe well above -20 °C, which is the lowest operating temperature of many common sensors, for up to about an hour of cryogen flow.



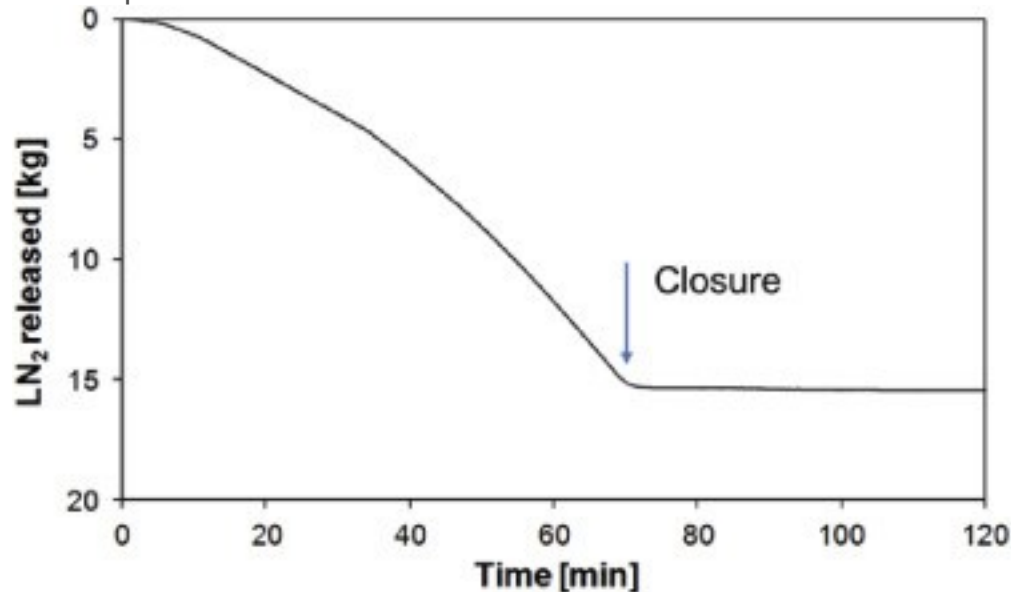
1. [Download high-res image \(238KB\)](#)

2. [Download full-size image](#)

Fig. 10. Stand-off pipe placed vertically to support measurements of [borehole](#) pressure.

2.3.3. Liquid nitrogen consumption

The amount of LN leaving the dewar and flowed through a borehole is monitored by placing the dewar on an electronic balance. Typical data for liquid nitrogen consumption over time is shown in [Fig. 11](#). The plot of LN consumption and time is flatter in the early stage, and then the slope becomes steeper as stimulation time increases. This nonlinear behavior corresponds to the strong vaporization in the dewar outlet, transport lines, and boreholes at earlier times, and gradual decrease of vaporization as the system cools down. Vaporization in the transport lines hinders flow, thus decreasing LN consumption rate.



1. [Download high-res image \(117KB\)](#)

2. [Download full-size image](#)

Fig. 11. Typical [liquid nitrogen](#) consumption vs. time.

2.4. True-triaxial loading equipment

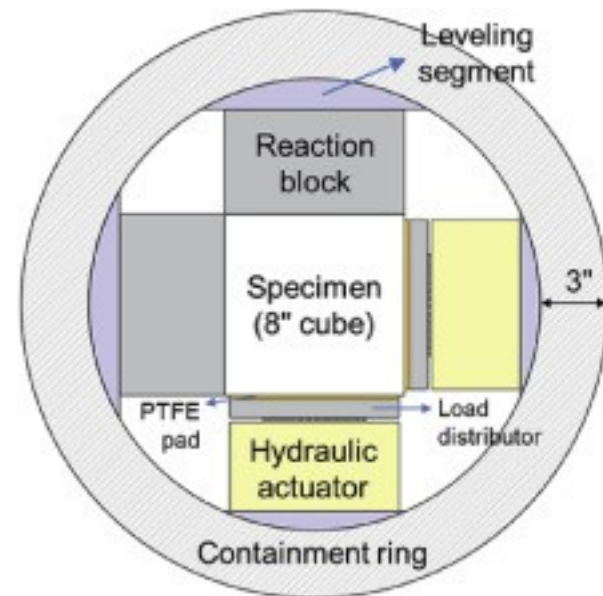
A true-triaxial loading system was developed to simulate effects of stress levels and stress [anisotropy](#) on the characteristics of cryogenic fracturing. A large specimen size (20 cm × 20 cm × 20 cm) was selected to create the sufficient thermal gradient required for thermal tensile fracturing.

2.4.1. Triaxial loading device

Commercially available true-triaxial load devices are closed-chamber systems, in which specimens and often [hydraulic actuators](#) are contained a sealed chamber, and not rated for operating at cryogenic temperatures. The closed-chamber system can create complications in design due to issues in thermal compatibility arising from large temperature differences between the specimen and the loading system, and accidental cryogen leakage through fractured specimens and transport lines. Therefore, we adopted and built an open system, which allows easier instrumentation and observations, and safer tests ([Fig. 12](#)). A drawback is that the system cannot apply [pore](#) fluid pressure to a specimen.



(a)



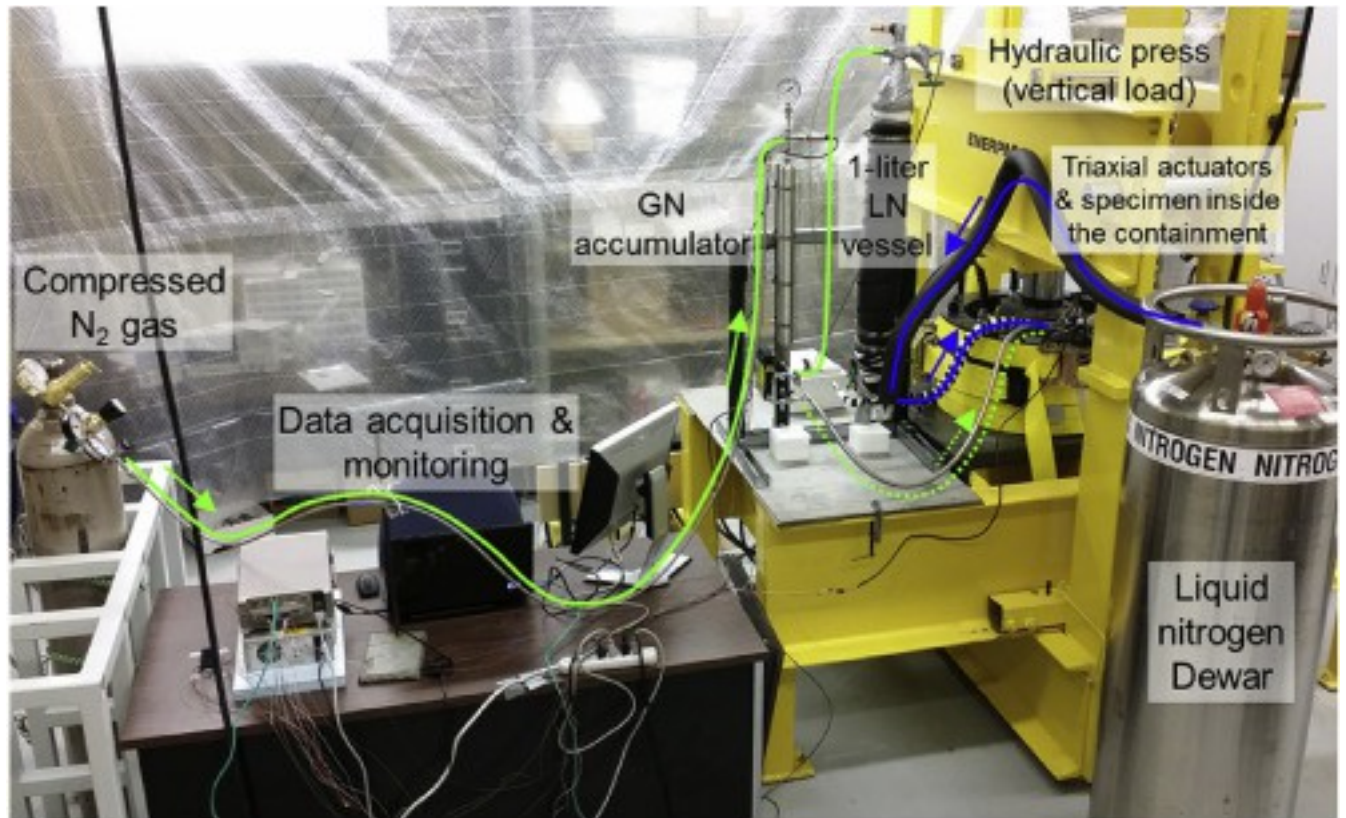
(b)

1. [Download high-res image \(617KB\)](#)
2. [Download full-size image](#)

Fig. 12. True-triaxial loading system. (a) Actuators and a specimen (not visible) inside the containment ring mounted on the press bed frame. Loading axes and specimen face numbers are indicated. (b) Plan view of the components laid in the containment.

The containment was designed for the selected specimen size 20 cm × 20 cm × 20 cm ([Fig. 12](#)). The triaxial loading (TX) system can load the specimen up to 30 MPa in x- and y-axes (using Enerpac RSM-1,500 cylinders), and 40 MPa in the z-axis (using Enerpac RR-20013), and can independently control loadings in the three axes. The two hydraulic pistons for x- and y-axes and the hydraulic press for z-axis were powered by three [pneumatic](#) hydraulic pumps. Three heavy-duty ratchet tie-down straps (2,300-kgf capacity each) surround the containment ring in case the containment ring yields. One of the procedural advantages of the system was the vertical loading frame can be

removed by rolling it away after unlocking it from the bed. This ability provides a user with space to work on specimens and inside the containment without moving the containment and items inside. The exposed system helps to better deal with any unexpected situation such as a cryogen spill and with instrumentation ([Fig. 12](#)). Because our system was quasi-static, an automatic servo [control system](#) for load control was not required. Constant forces can be maintained by either manual control or in a quasi-automatic manner using pressure relief valves attached to the hydraulic lines. In the manual control, whenever more than a certain amount of natural decay of pressure occurred in the hydraulic system, the hydraulic pressure was increased. Our hydraulic system can make use of pressure relief valves in the hydraulic lines to quasi-automatically control constant pressure, which needs less attention than the manual control. [Silicone](#) or PTFE pads were placed between rock specimens and the loading pad to provide uniform contacts and loading to specimen surface ([Fig. 12](#)). PTFE and silicone pads resist temperature down to $-212\text{ }^{\circ}\text{C}$ and $-62\text{ }^{\circ}\text{C}$, respectively. [Fig. 13](#) shows a picture of a laboratory apparatus fully assembled for cryogenic stimulation experiments under specimen triaxial confining load, with controllable LN flow rate through boreholes, GN pressurization, and monitoring of environmental parameters. The detailed schematics including connected lines and valves for [flow control](#) for the setup are presented in [Fig. 3](#).

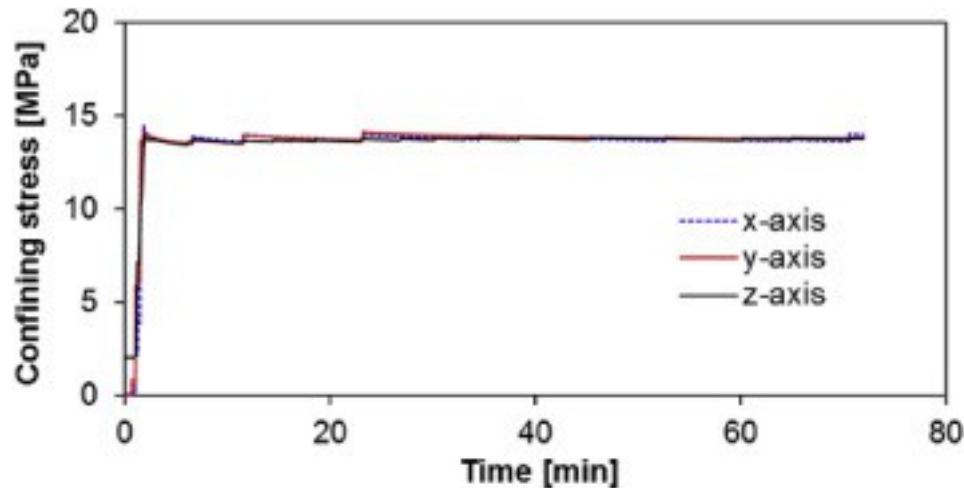


1. [Download high-res image \(1MB\)](#)
2. [Download full-size image](#)

Fig. 13. Assembled setup for [cryogenic](#) stimulation tests under specimen confining load. Green lines are tubes for pressurized gas nitrogen and blue lines are for tubes for [liquid nitrogen](#). (For interpretation of the references to colour in this figure legend, the reader is referred to the web version of this article.)

2.4.2. Triaxial loading performance tests

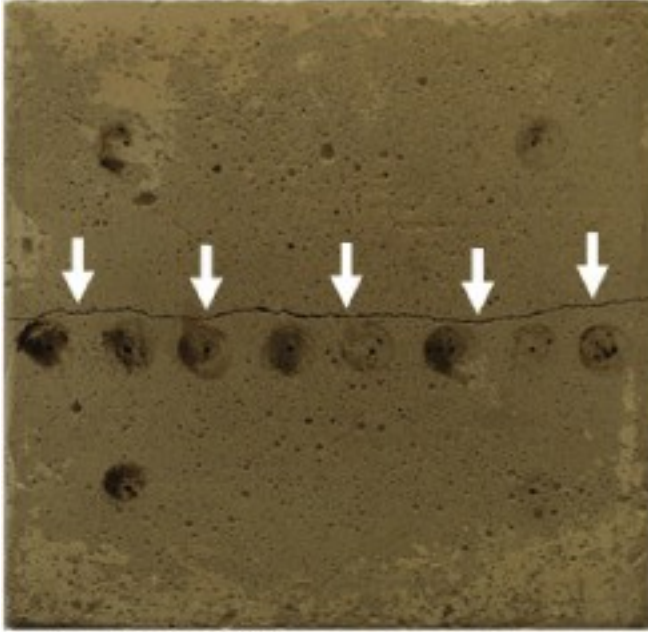
A constant force was maintained by the manual control in the test shown in [Fig. 14](#). Discontinuities in the plots represent hydraulic pumps applied to make up for pressure decay. The manual control can be more accurate than quasi-automatic control, but requires more frequent updates. Note that the test in [Fig. 14](#) was manually controlled having an error of $\pm 2\%$. Forces exerted by the hydraulic pistons were calculated by multiplying hydraulic pressure in the hydraulic lines measured using pressure transducers by the effective area of hydraulic pistons. Then the specimen stresses were obtained by dividing the piston forces by the specimen surface areas.



1. [Download high-res image \(110KB\)](#)
2. [Download full-size image](#)

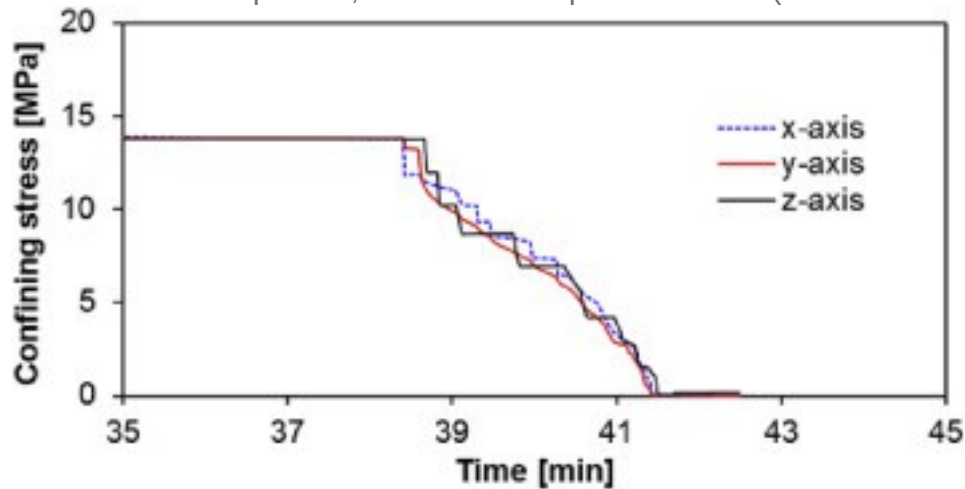
Fig. 14. Confining load tests – manual control of constant stress (isotropic 14 MPa). Silicone pads were placed between the specimen surface and loading plates to accommodate for irregularities in the surface. The silicone pads appeared to function well in distributing the load on slightly uneven specimens. We did not observe any specimen damage after loading up to the maximum isotropic stress of 30 MPa. The top surfaces of our samples were rougher, and the silicone pads help distribute load over the surfaces. The pads were inevitably extruded out of the contact against rough surfaces at high confining stress, and damaged. As laboratory cryogenic stimulations were relatively short-term (less than an hour), the temperature rating ($-62\text{ }^{\circ}\text{C}$) of the silicone pads was sufficient as the block surface remained above this temperature. PTFE sheets are stiffer than the silicone pads, but malleable enough at high pressure to accommodate any reasonably undulating surfaces, and have good temperature rating down to $-212\text{ }^{\circ}\text{C}$. Because the PTFE is stiffer, it may not properly distribute the load over the entire area when the specimen is undulating more than a certain level.

In one of loading tests that we performed, acute anisotropic stress conditions were created in the specimen due to abrupt, non-synchronized unloading in three axes. The specimen was subjected to an anisotropic condition where x- and y-axes were loaded to $\sim 14\text{ MPa}$ and z-axis was loaded to $\sim 0\text{ MPa}$ due to unsynchronized rapid unloading for a couple of times (each time the anisotropic condition lasted about 0.5 s). This created prominent fractures at the center of the specimen perpendicular to the z-axis (Fig. 15). After this observation, we devised to make use of pressure relief valves (Enerpac V-152) to simultaneously and slowly unload the three axes as shown in Fig. 16.



1. [Download high-res image \(319KB\)](#)
2. [Download full-size image](#)

Fig. 15. Prominent fracture along the centers at the sides in a concrete specimen created due to repeated, acute anisotropic conditions (sudden unloading of z-axis only).



1. [Download high-res image \(117KB\)](#)
2. [Download full-size image](#)

Fig. 16. An example of synchronized unloading to avoid large stress [anisotropy](#), using pressure [relief valves](#) in the [hydraulic system](#).

3. Experimental procedure

[Cryogenic](#) stimulation is performed by flowing LN from its dewar into [boreholes](#) of specimens and then flowing gaseous nitrogen out. Baseline measurements of rock conditions relevant to fracture indication were done before any treatment, and then the

same measurements were performed during treatments or after completing the treatments for comparison. Fracture assessments included [acoustics](#), pressure decay tests, breakdown fracturing, visual inspection, and [X-ray](#) computed [tomography](#) (CT).

3.1. Procedure

As mentioned previously, a constant supply of LN is needed to cool the rock and any stagnant condition will cause a rapid increase in the borehole temperature. Thus, [liquid nitrogen](#) is continuously flowed through the borehole. Using our cryogenic fracturing apparatus under triaxial loading conditions, we perform two different cryogenic stimulation schemes. The first one is low-pressure liquid nitrogen flow, where liquid nitrogen is directly flowed from the dewar by a pressure difference between the inside of the dewar and outside the dewar upon opening the dewar's release valve. Pressure ranges from 35 to 135 kPa (gauge pressure) in the borehole, depending on the [internal pressure](#) level inside the dewar.

The other scheme was high-pressure LN flow, where liquid nitrogen was flowed through the borehole under higher pressure (2–2.8 MPa) for faster cooling in the borehole due to faster flow rate and reduced film boiling thickness. In a high-pressure liquid nitrogen flow, the higher [fluid pressure](#) facilitates fracture opening by helping to reach the [tensile strength](#) of the rock. Because the vessel storing liquid nitrogen for higher-pressure injection is small (1 L) ([Fig. 4](#)), normally we apply the higher-pressure stimulation multiple times, and each stimulation cycle is brief (1–2 min).

3.2. Fracture characterization

Fracture assessments are carried out by borehole pressure decay, specimen breakdown pressure, and [acoustic measurements](#). The borehole pressure decay is performed by applying pressure to the borehole, shutting the borehole in, and monitoring the pressure decay. This is tested before cryogenic treatments to provide a baseline and then tested between treatments and after completing the treatments for comparison. After all planned stimulations are completed for a specimen, the specimen is subject to gas nitrogen (GN) pressure to fully fracture (“breakdown”) the specimen. These breakdown pressures are compared to baseline breakdown pressure of an untreated specimen, and also with those of specimens that were treated in different conditions. Breakdown tests are done at the last stage after all other tests and measurements are completed as it fully fractures the block to the surface. [Elastic wave](#) propagation is measured using [ultrasonic transducers](#) before and after the treatments. The post-stimulation ultrasonic measurements are done before applying

breakdown pressure so that we can assess the effect of cryogenic stimulations. Elastic waves are governed by the mechanical properties of the medium. In particular, the [wave velocity](#) in jointed rock masses is a function of the density of fractures ([Cha et al., 2009](#)). When other properties such as intact rock properties, density, and joint [stiffness](#) are the same, the wave velocity can be used as a monitoring tool for fracture generation. Also, CT scanning is performed for fracture assessment before and after stimulations.

3.3. Specimen preparation

[Shale](#) and [sandstone](#) were collected from [outcrops](#) of producing formations. A large specimen size (20 cm × 20 cm × 20 cm) was selected in order to create sufficient thermal gradient in the specimen for an extended time. Collected [rock blocks](#) were precisely cut into 20 cm × 20 cm × 20 cm cubic shapes using a laser-guided bridge saw. Then a 2.5-cm diameter wellbore was drilled by using a diamond imbedded coring [drill bit](#) with the 2.6-cm outer diameter to a depth of 15 cm. Following drilling, a 2.5-cm stainless steel-316 tube (casing) was attached to the wellbore by applying epoxy, after the [thermocouples](#) were placed inside the wellbore. The casing extends 5 cm into the wellbore ([Fig. 8a](#)). Mortar concrete blocks were also used for specimens as surrogates for real rocks. Fresh concrete with a water to cement ratio of 0.55, and sand to cement ratio of 2.5 was poured into a 20 cm × 20 cm × 20 cm mold and sealed in a plastic bag. After 24 h, the seal and mold were removed, and the concrete was cured under water ([ASTM, 2014a](#)).

Index properties of intact samples were obtained for test specimens. Permeability and [porosity](#) were measured using a CMS 300 (CoreLab). Elastic constants were obtained from measurements of elastic wave velocities ([ASTM, 2008b](#), [Cha and Cho, 2007](#)). [Specific heat](#) capacity was obtained by using a [calorimeter](#). Splitting tensile strength and unconfined uniaxial [compressive strength](#) were obtained using procedures from the ASTM standards ([ASTM, 2008a](#), [ASTM, 2014b](#)).

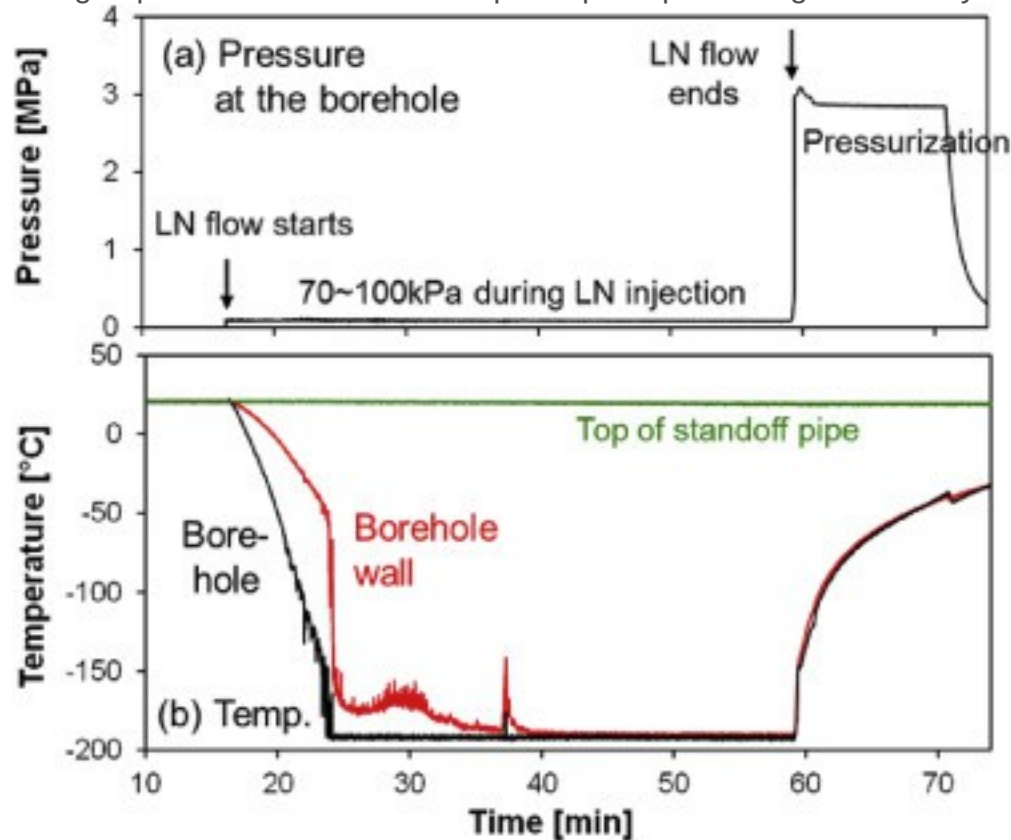
4. Laboratory performance and fracture assessment

Following the procedures explained earlier, we performed [cryogenic](#) stimulation experiments using low-pressure and higher-pressure LN flow. Temperature and pressure behaviors for some tests in and around [borehole](#) are presented, followed by assessments of generated fractures for a low-pressure LN stimulation.

4.1. Low- and high-pressure liquid nitrogen flow-through

In the low-pressure LN flow scheme, LN was injected until after borehole wall was fully cooled down to the nitrogen [boiling point](#) ([Fig. 17](#)). When the low-pressure LN flow was

stopped, gas nitrogen pressure was applied to the borehole, pressurizing it at about 3 MPa (Fig. 17). During the pressurization period (about 20 s), rapid temperature increase was observed following the adiabatic compression of gas (Fig. 17b). This gas nitrogen pressure was in an attempt to open up cracks generated by the [thermal shock](#).



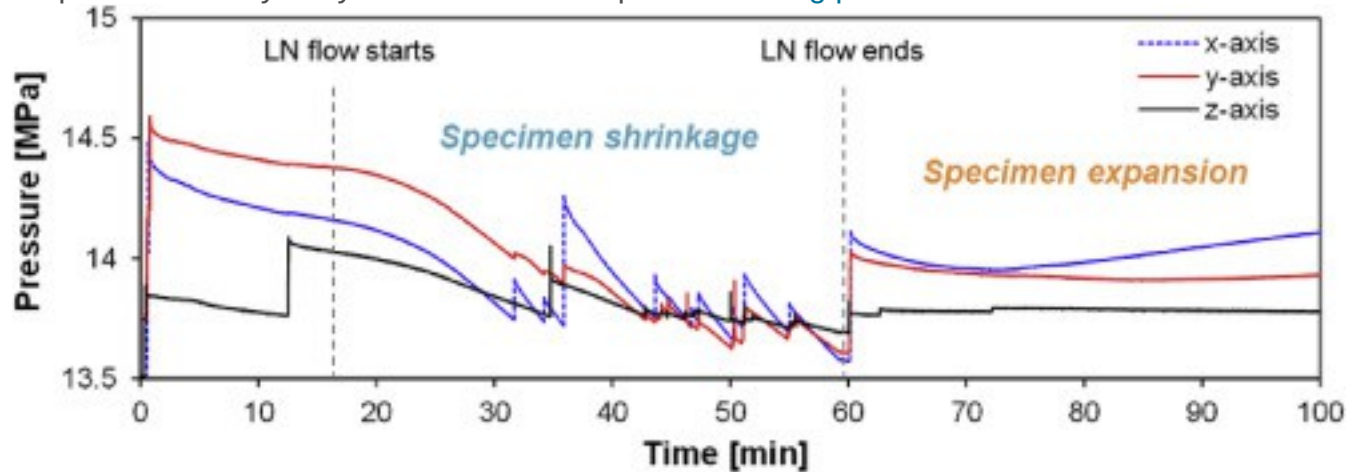
1. [Download high-res image \(293KB\)](#)
2. [Download full-size image](#)

Fig. 17. [Borehole](#) pressure and temperature during low-pressure LN flow followed by borehole pressurization in a concrete specimen under 14 MPa isotropic confining stress.

The sudden drop in the temperature on borehole wall surface (at 24 min - Fig. 17b) may indicate a fluid transition to the [liquid phase](#) in the borehole. However, the boiling at the borehole wall surface continued for more than 20 min after that, as we see that the borehole wall did not reach nitrogen boiling point for an extended time.

Contraction and expansion of specimens were observed from pressure responses of the [hydraulic system](#) (Fig. 18). When the specimen was cooled down, the specimen shrank, and the pistons in contact with the specimen lost pressure at a faster rate than at the steady-state condition. When the temperature of the specimen increases, the specimen expands, and the piston pressure starts to increase, making the hydraulic

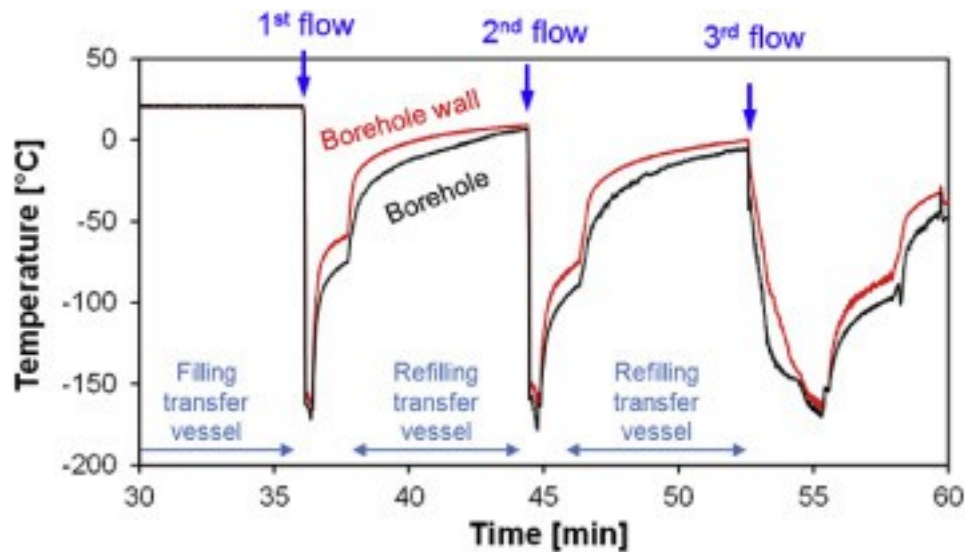
pressure increase. In [Fig. 18](#), each jump represents a manual adjustment to make up for pressure decay in hydraulic lines to keep the [confining pressure](#) ~14 MPa.



1. [Download high-res image \(251KB\)](#)
2. [Download full-size image](#)

Fig. 18. Shrinkage and expansion of a concrete specimen due to specimen cooling and warming, indicated from hydraulic pressure responses during low-pressure LN flow (followed by pressurization).

In the higher-pressure LN flow scheme, the cryogen pressures in a borehole during flow range from 2 to 5 MPa. [Liquid nitrogen](#) flowing through the borehole under higher pressure (thus higher flow rate) decreases borehole [surface temperature](#) more quickly than for the low-pressure treatment ([Fig. 19](#)) probably due to faster heat exchange and more suppressed surface vapor [cushion](#). Therefore, thermal shock becomes more efficient because of the higher cooling rate. In our higher-pressure LN flow, the stimulation was applied multiple times. This was because the volume of the high-pressure LN transfer vessel was small (1 L), which makes each stimulation brief (e.g., 1–2 min). Higher-pressure stimulation may also help open up fractures created by thermal shock.



1. [Download high-res image \(222KB\)](#)
2. [Download full-size image](#)

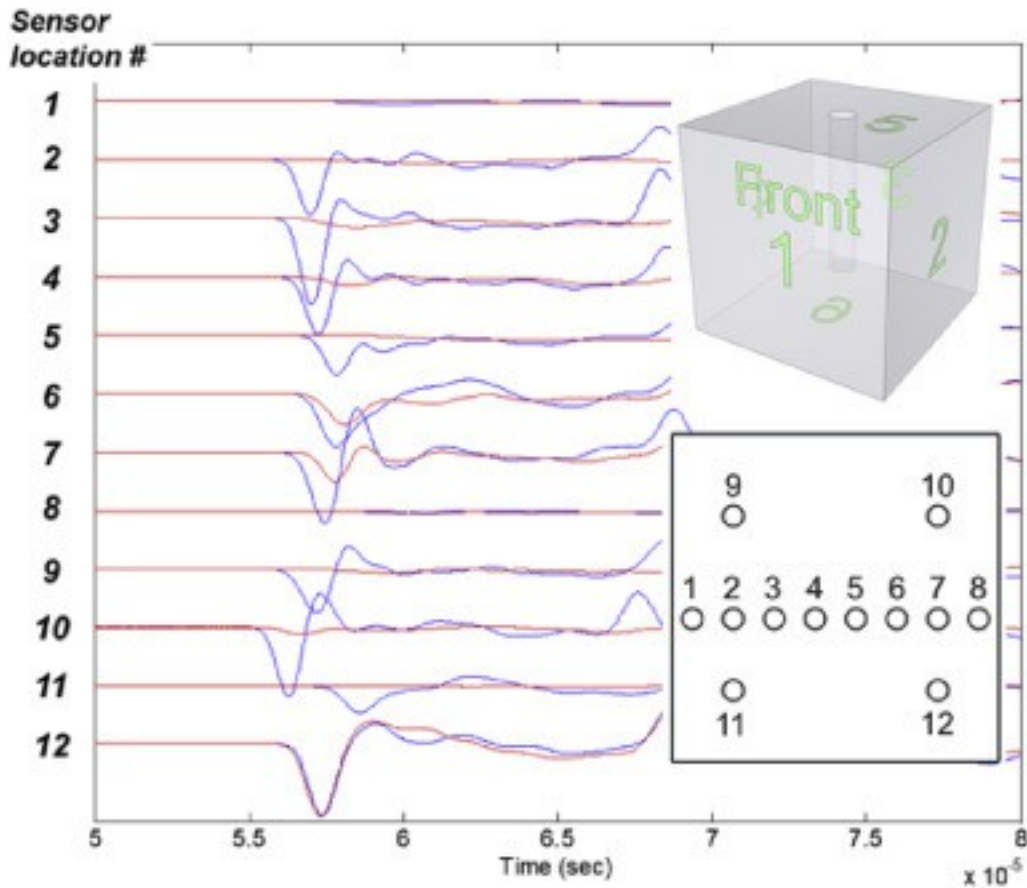
Fig. 19. Temperature changes during multiple higher-pressure LN flow-through.

4.2. Fracture assessment and characterization

Methods applied to check whether fractures have been created by cryogenic stimulations include the pressure decay, [acoustic waves](#), CT, and breakdown fracturing.

4.2.1. Acoustic waves

[Elastic wave](#) data were collected to obtain parameters on changes in specimen [stiffness](#) and quality by waveform comparisons. [Acoustic](#) signals were measured between Faces 1&3 and 2&4 (pairs of opposing faces). For each set of faces, [acoustic measurements](#) were conducted at twelve locations ([Fig. 20](#)). We observed that [acoustic velocities](#) and amplitudes decrease after cryogenic stimulations, indicating fracture creation in the specimens. The amplitudes and velocities decreased significantly in the areas comprising #2, 3, 4, and 5, indicating that major cracks exist there. On the other hand, the area in the lower right corner remained relatively intact (#12) ([Fig. 20](#)). Results of acoustic measurements on post-stimulation specimens prior to breakdown tests generally agree with the fracture profile found after the breakdown tests. This indicates that initial “seed” fractures created by cryogenic stimulations are extended during breakdown tests.



1. [Download high-res image \(323KB\)](#)
2. [Download full-size image](#)

Fig. 20. An example of P-wave signatures before (blue lines) and after (red lines) liquid nitrogen treatment in a concrete specimen (wave transmission between Faces 1&3). (For interpretation of the references to colour in this figure legend, the reader is referred to the web version of this article.)

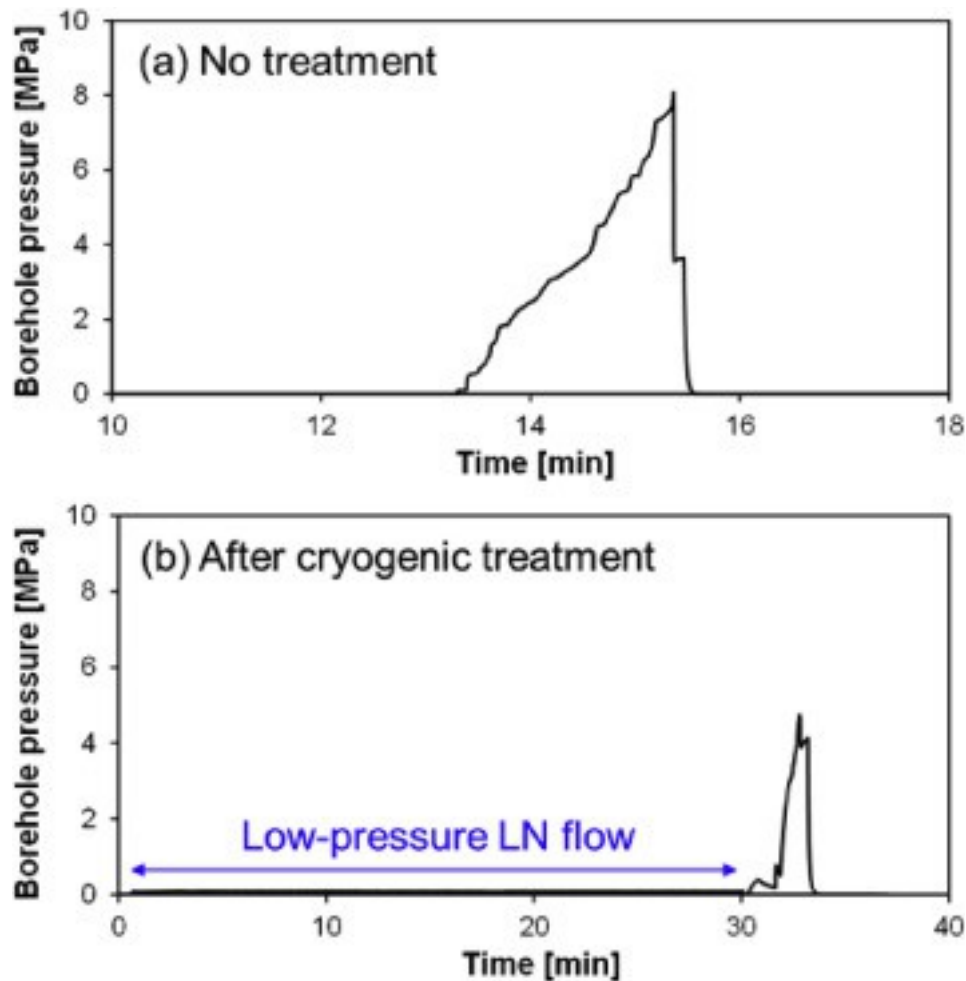
4.2.2. Borehole pressure decay

Permeability enhancement was assessed by comparing pressure decay tests before and after cryogenic stimulation. Pressure decay test results show that the low and high-pressure liquid nitrogen stimulations increase the permeability of stimulated specimens. In one test, low-pressure LN flowed for 30 min resulted in a significant increase in permeability indicated by a rapid pressure decay. Cycles of higher-pressure stimulation under triaxial loading also led to significant permeability enhancements. It was found that specimen temperature and confining stress play noticeable roles in pressure decay results. Detailed pressure decay results and analysis are reported in [Alqatahni et al. \(2016\)](#). The pressure decay results allow only relative, qualitative comparisons.

With [numerical analysis](#) and geometrical consideration, quantitative estimation of averaged permeability of a block may be obtained.

4.2.3. Post-stimulation breakdown fracturing

After cryogenic stimulation and other assessments are completed for a specimen, the specimen is subjected to increasing gas nitrogen (GN) pressure until the block fully fractures (“breakdown”) all the way to the outer surfaces of the block. [Water pressure](#) cannot be used for breakdown tests because water will freeze due to cold temperature. Rock fracturing by [gas pressure](#) involves more safety considerations than hydraulic fracturing due to the much larger compressibility of nitrogen gas. In our laboratory tests, specimens were fully contained under triaxial load so that upon fracturing nothing was ejected. The breakdown pressures are compared with baseline breakdown pressure of untreated specimen ([Fig. 21a](#)). A result shows that cryogenic treatment by low-pressure liquid nitrogen flow-through decreases the breakdown pressure level by more than 40% ([Fig. 21](#)). The significantly reduced breakdown pressure may make field stimulation by gas fracturing using high-pressure gaseous nitrogen more economical and safer.



1. [Download high-res image \(217KB\)](#)
2. [Download full-size image](#)

Fig. 21. Post-stimulation breakdown fracturing of a concrete specimen by nitrogen [gas pressure](#).

4.2.4. X-ray computed tomography

Proppants were not used in this study. Fractures created by cryogenic stimulations tended to close as a specimen warms up. No self-propping mechanisms were found in laboratory-sized specimens of concrete, [shale](#), and [sandstones](#). Consequently, scanning with [X-ray](#) CT with voxel size 0.2 mm × 0.2 mm × 0.2 mm failed to provide enough resolution to identify cracks generated near the wellbore.

5. Conclusions

We built an experimental system for [cryogenic](#) fracturing study under true-triaxial loading conditions, in a controlled laboratory environment that resembles “downhole” conditions. The apparatus consists of a true-triaxial loading device, a [liquid](#)

[nitrogen](#) delivery and [borehole](#) flow-through system, and a measurement/characterization system. The true-triaxial loading system can load to reservoir confining stress levels on 20 cm cubic blocks, independently control load in the three axes, and keep constant [effective stresses](#) on specimens. The design of the loading components and specimen being placed in an exposed chamber allows thermal compatibility and instrumentation. Unlike pressure-based fracturing technology, the flow must be ensured to maximize [thermal shock](#). Flow through borehole is allowed by “coaxial” flow path, where cryogen enters borehole through central inlet tube and outflow through the [annulus](#). The cryogen can be delivered to a borehole under low pressure directly from a dewar and under higher pressure from a transfer vessel. Boreholes may be pressurized by gas after the thermal stimulation to study synergistic effects. To characterize thermally induced fractures, [acoustics](#), pressure decay tests, and breakdown fracturing were applied, and able to effectively capture created fractures and permeability changes.

Data were gathered from cryogenic tests on triaxially stressed rock cubes proves that the system works adequately (More data available in [Alqahtani \(2015\)](#)). With the experimental system developed, high-quality data can be gathered to provide a deeper understanding of cryogenic fracturing and advance the cryogenic fracturing processes toward successful field applications. As waterless or reduced-water [well stimulation](#) technologies are sought more than ever, the cryogenic stimulation may be studied systematically in laboratories.

Acknowledgements

Support for this research was provided by Research Partnership to Secure Energy for America (RPSEA) (Grant no. [10122-20](#)). Work by TJK was performed at Lawrence Berkeley National Laboratory (LBNL) of the US Department of Energy (DOE) under Contract No. DE-AC02-05CH11231. Funding for this project is provided by Research Partnership to Secure Energy for America (RPSEA) through the Ultra-Deepwater and Unconventional Natural Gas and Other [Petroleum](#) Resources program authorized by the US [Energy Policy](#) Act of 2005. RPSEA is a nonprofit corporation whose mission is to provide a stewardship role in ensuring the focused research, development, and deployment of safe and environmentally responsible technology that can effectively deliver [hydrocarbons](#) from domestic resources to the citizens of the US. RPSEA, operating as a consortium of premier US energy research universities, industry, and independent research organizations, manages the program under a contract with DOE's National [Energy Technology](#) Laboratory.

References

[Alqahtani, 2015](#)

N.B. Alqahtani **Experimental Study and Finite Element Modeling of Cryogenic Fracturing in Unconventional Reservoirs**

(Ph.D. Dissertation)

Colorado School of Mines. Arthur Lakes Library (2015)

[Alqatahni et al., 2016](#)

Alqatahni, N.B. et al., 2016. Experimental Investigation of Cryogenic Fracturing of Rock Specimens under True Triaxial Confining Stresses, SPE Europec featured at 78th EAGE Conference and Exhibition, Vienna, Austria, 30 May–2 June 2016. SPE-180071-MS.

[ASTM, 2008a](#)

ASTM **ASTM D3967 Standard Test Method for Splitting Tensile Strength of Intact Rock Core Specimens**

(2008)

[ASTM, 2008b](#)

ASTM **D2845–08 Standard Test Method for Laboratory Determination of Pulse Velocities and Ultrasonic Elastic Constants of Rock**

ASTM International (2008)

[ASTM, 2014a](#)

ASTM **ASTM C192/C192M Standard Practice for Making and Curing Concrete Test Specimens in the Laboratory**

(2014)

[ASTM, 2014b](#)

ASTM **ASTM D7012 Standard Test Methods for Compressive Strength and Elastic Moduli of Intact Rock Core Specimens under Varying States of Stress and Temperatures**

(2014)

[Cha et al., 2016](#)

Cha, M. et al., 2016. Studying cryogenic fracturing process using transparent specimens, The 1st International Conference on Energy Geotechnics, August 29-31, 2016, Kiel, Germany, pp. 211–216.

[Cha and Cho, 2007](#)

M. Cha, G.C. Cho **Compression wave velocity of cylindrical rock specimens: engineering modulus interpretation**

Jpn. J. Appl. Phys. Part 1 Regul. Pap. Brief Commun. Rev. Pap., 46 (7B) (2007), pp. 4497-4499

[CrossRefView Record in Scopus](#)

[Cha et al., 2009](#)

M. Cha, G.C. Cho, J.C. Santamarina **Long-wavelength P-wave and S-wave propagation in jointed rock masses**

Geophysics, 74 (5) (2009), pp. E205-E214

[CrossRefView Record in Scopus](#)

[Cha et al., 2014](#)

M. Cha, *et al.* **Cryogenic fracturing for reservoir stimulation – laboratory studies**

J. Pet. Sci. Eng., 124 (0) (2014), pp. 436-450

[ArticleDownload PDFView Record in Scopus](#)

[Grundmann et al., 1998](#)

S.R. Grundmann, G.D. Rodvelt, G.A. Dials, R.E. Allen **Cryogenic nitrogen as a hydraulic fracturing fluid in the devonian shale**

SPE-51067-MS

SPE Eastern Regional Meeting, Society of Petroleum Engineers, Pittsburgh, Pennsylvania(1998)

[Mazza, 1997](#)

R.L. Mazza **Liquid CO2 Improves Fracturing. Hart's Oil and Gas World**

(1997), p. 22

[McDani](#)

[el et al.,](#)

[1997](#)

B.W. McDaniel, S.R. Grundmann, W.D. Kendrick, D.R. Wilson, S.W. Jordan **Field applications of cryogenic nitrogen as a hydraulic fracturing fluid**

SPE 38623

SPE Annual Technical Conference and Exhibition, Society of Petroleum Engineers, Inc., San Antonio, Texas (1997)

Copyright 1997

[S](#)
[t](#)
[r](#)
[i](#)
[n](#)
[g](#)
[f](#)
[e](#)
[l](#)
[l](#)
[o](#)
[w](#)
[-](#)
[e](#)
[t](#)
[-](#)

W.T. Stringfellow, J.K. Domen, M.K. Camarillo, W.L. Sandelin, S. Borglin **Physical, chemical, and biological characteristics of compounds used in hydraulic fracturing**

J. Hazard. Mater., 275 (2014), pp. 37-54

[ArticleDownload](#) [PDFView](#) [Record in Scopus](#)

[Wang](#)
[et al.,](#)
[2016](#)

L. Wang, *et al.* **Waterless fracturing technologies for unconventional reservoirs- opportunities for liquid nitrogen**

J. Nat. Gas Sci. Eng. 35 Part A (2016), pp. 160-174

[ArticleDownload](#) [PDFView](#) [Record in Scopus](#)

[Wilson et al.,](#)
[1995](#)

Wilson, D.R., Siebert, R.M. and Lively, P., 1995. Cryogenic Coal Bed Gas Well Stimulation Method. Google Patents.